

Molecular Dynamics Studies of the Kinetics of Freezing of (NaCl)₁₀₈ Clusters

Jinfan Huang, Xiaolei Zhu, and Lawrence S. Bartell*

Department of Chemistry, The University of Michigan, Ann Arbor, Michigan 48109

Received: November 17, 1997; In Final Form: February 18, 1998

Molecular dynamics simulations adopting the Born–Mayer–Huggins potential function were performed on a series of (NaCl)₁₀₈ clusters to observe their properties during heating and cooling and to monitor their nucleation events during freezing. Melting was found to be considerably sharper than that of clusters of softer materials whose solid form, unlike that of salt, is well-wetted by the melt. The resulting liquid clusters were observed to be greatly distorted from a spherical shape by capillary waves. The freezing of highly supercooled liquid clusters was found to be in qualitative accord with the classical theory of homogeneous nucleation. Moreover, the interfacial free energy parameter σ_{sl} inferred via nucleation theory, namely, 117.7, 117.6, and 119.6 mJ/m² at 500, 525, and 550 K, respectively, was close to the value predicted by the empirical Turnbull relation and in crude agreement with an experimental value determined at a much lower degree of supercooling and derived on a very different basis. Nevertheless, the thickness of the interface between the liquid and solid implied by Granasy's diffuse interface theory and by density functional calculations was so large in comparison with the radius of the critical nucleus according to the classical theory as to cast considerable doubt about the quantitative applicability of that theory to the present clusters. On the other hand, the MD nucleation rates, taken together with the prior and somewhat speculative experimental result, indicate that the classical theory performs better than the diffuse interface theory. Calculations and possible experiments to clarify the situation are outlined.

Introduction

In proportion to its importance in science and technology, homogeneous nucleation in condensed phases has received comparatively little attention in the research laboratory. Until a half-century ago, when Turnbull and his colleagues^{1–4} showed how meaningful experiments could be carried out to measure nucleation rates in freezing with a fair probability that the nucleation was genuinely homogeneous, virtually no experimental information existed. Because Turnbull's technique, when fully implemented, is difficult and does not lend itself to routine investigations, it was felicitous to find an alternative technique for monitoring nucleation rates, not only in freezing^{5–9} but also in some solid-state transitions.¹⁰ The subjects are large molecular clusters generated in rapidly cooling supersonic expansions and monitored by electron diffraction. Although both of the experimental methods can follow nucleation dynamics, neither is able to observe the transformations in molecular detail. A technique which has this capability, however, is that of computer simulation.¹¹ Molecular dynamics (MD) calculations have already provided important information about the freezing of atomic liquids. Swope and Andersen,¹¹ in particular, carried out massive computations at an IBM laboratory on systems as large as one million atoms and found that the nucleation spontaneously taking place in their system was at least qualitatively in accord with the classical theory of homogeneous nucleation. They also found that bulk systems simulated with fewer atoms by imposing periodic boundary conditions gave spurious results for systems smaller than perhaps 400–4000 atoms, putting the study of nucleation in bulk systems beyond the resources of ordinary laboratories.

Computational research^{12,13} was initiated in this laboratory to complement the study of nucleation in supersonic jets of

clusters. Our simulations have focused on clusters with free boundaries rather than systems subject to periodic boundary conditions in order to avoid the aforementioned problems and to work with systems small enough to be carried out on workstations. Even though van der Waals clusters of atoms smaller than a few thousand atoms do not pack in the same way as atoms in bulk matter,¹⁴ the properties of cores of much smaller clusters of the polyatomic molecules we have examined have quite faithfully conformed with those of the bulk.^{13,15} Of course, with such small systems there is some uncertainty in the cluster volume that can be considered to be eligible for nucleation. More will be said about this subsequently. Until now, as far as we are aware, simulations of nucleation in condensed matter have all been carried out on simple atomic¹⁶ or on nonpolar molecular systems.^{13,17,18} These systems have differed from the present system, salt, in that the solid has been well-wetted by the melt. In such cases, the surface tends to melt before the core as the clusters are heated and nucleation always occurs in the interior during cooling. With simple salts, as shown by Rose and Berry,¹⁹ the melt does not spontaneously wet the surface and melting tends to be sharper. What effect such differences have on nucleation is uncertain.

For the above reasons it seemed worthwhile to carry out an exploratory MD study of nucleation in clusters of sodium chloride. Experiments for comparison are available from the research of Buckle and Ubbelohde^{20–22} who froze microdrops of various salts produced in a heated cloud chamber. In addition, Rose and Berry have performed MD simulations of the melting and freezing characteristics of clusters of KCl ranging up to 32 KCl pairs.¹⁹ Such clusters, however, appear to be too small to experience a significant free energy barrier to freezing. Luo, Landmann, and Jortner²³ also investigated

TABLE 1: Potential Parameters Adopted for NaCl

	pair		
	Na ⁺ –Na ⁺	Na ⁺ –Cl [−]	Cl [−] –Cl [−]
A^a	4.255×10^{-20}	3.380×10^{-20}	2.535×10^{-20}
σ^b	0.2340	0.2755	0.3170
ρ^b	0.0317	0.0317	0.0317

^a J/molecule. ^b nm.

the dynamics of salt clusters ranging up to (NaCl)₁₀₈ but did not report any observations of nucleation. On the other hand, our molten (NaCl)₁₀₈ clusters consistently underwent homogeneous nucleation on cooling before they froze. We report our preliminary findings in the following.

Computational Details

Simulations. Molecular dynamics simulations were carried out on an IBM RISC workstation with a modified version of the program MDIONS²⁴ incorporating the leapfrog algorithm. Time steps of 8 fs were used in all computations. The well-known Born–Mayer–Huggins interaction potential function^{25,26} for ions separated by the distance r_{ij} , or

$$U = \sum_{ij} \{q_i q_j r_{ij}^{-1} + A_{ij} \exp[(\sigma_{ij} - r_{ij})/\rho]\} \quad (1)$$

was adopted. Values of the constants A_{ij} , σ_{ij} , and ρ taken from Tosi and Fumi²⁷ are listed in Table 1. Configurational energies depended strongly on the shape of a cluster, the most stable shape found being that of a simple cube with an internal fcc packing of ions corresponding to the rock salt structure. Initial configurations were assigned a lattice constant of 5.641 Å, the experimental value at 299 K.²⁸

Heating runs to generate caloric curves and to prepare melts for the nucleation runs began with the cluster in its cubic starting configuration in a heat bath at 298.15 K for 10 000 time steps followed by 15 000 steps at constant energy. A series of heating stages at 20 K increments began at 320 K. At every stage the cluster spent 1000 steps in a heat bath (i.e., stage in which velocities were rescaled at each step in order to approach the desired temperature). Following each heating stage were 4000 steps at constant energy. This rapid rate of change of temperature was slow enough to establish a near-equilibrium at temperatures not too close to the melting temperature but was clearly too fast in the vicinity of the transition. Therefore, additional runs were carried out that allowed 10 000 time steps in the bath plus 4000 at constant energy per 20 K increment close to the transition to provide a better estimate of the melting point. Heating was continued to 1100 K, a temperature 27 K above the bulk melting point. Because of the well-known size effect on melting, it was found that the cluster melted well before this temperature was reached. Indeed, one Na⁺Cl[−] pair of ions evaporated at 1020. Therefore, to begin cooling with a complete set of 108 pairs in the cluster, a configuration no hotter than 1000 K was taken as the high-temperature point.

Cooling runs were of two types. To acquire a cooling curve, a cluster was cooled 20 K at each stage, beginning with the 980 K stage, by the reverse of the heating process. The cooling rate, then, was 2.5×10^{11} K/s, a rate so rapid that a considerable supercooling was attained before freezing took place. Nevertheless, the rate allowed metastable equilibrium to be achieved well enough to yield a reasonable estimate of the difference in heat capacity between the highly supercooled liquid phase and the solid. This estimate is needed for later calculations of the free energy of freezing. The other type of cooling was for the

TABLE 2: Temperatures and Freezing Times in MD Nucleation Runs

500 K		525 K		550 K		N_0^a
run no.	t , ps	run no.	t , ps	run no.	t , ps	
1	18.0	10	17.6	12	20.0	15/16
9	21.6	14	22.4	8	28.0	14/16
16	22.0	9	22.8	14	31.2	13/16
8	24.4	4	25.6	7	38.4	12/16
11	25.2	15	28.0	11	43.2	11/16
4	29.6	2	28.8	2	54.8	10/16
15	34.8	8	29.6	16	56.0	9/16
6	35.6	16	34.0	1	72.4	8/16
2	36.8	7	36.0	13	76.4	7/16
3	38.4	11	42.4	15	87.6	6/16
13	39.6	1	47.2	9	88.0	5/16
12	43.2	4	52.8	3		4/16
10	50.8	6	53.2	4		3/16
5	50.8	3	68.8	5		2/16
7	58.4	13	71.2	6		1/16
13	59.6	12	72.8	10		0

^a Fraction of sample remaining liquid at time t .

purpose of determining nucleation rates. Rates were investigated at three temperatures, 550, 525, and 500 K, by immediately subjecting clusters at 1000 K to heat baths at the desired temperatures and keeping them in the heat baths during the entire nucleation process. Reasons for this will be discussed later. To generate 16 different candidates for nucleation runs at each temperature, the last stage at 1000 K before cooling in a given run was subjected to another 2000 time steps to produce a melt with a different history for the next nucleation run. How many time steps are required to generate truly independent initial conditions is an open question. If initial configurations are too highly correlated, nucleation times might be expected to bunch too closely and give an excessive nucleation rate. As can be seen in the nucleation events listed in Table 2, at least there is no discernible correlation between the sequence of nucleation times and the sequence of runs.

Conventions and Tests. Various diagnostic tests were applied to assess the heating and cooling runs including configurational energies, the Lindemann index δ ,^{29–32} pair correlation functions $g(r)$, and visual images of the clusters. Each test could readily distinguish between molten and crystalline clusters, but none were sufficiently sensitive to be able to identify possible seeds of the crystal left in the melt that might be able to act as nuclei for condensation. In parallel investigations of nucleation kinetics of several hexafluorides, it turned out that Voronoi polyhedra^{33,34} were able to identify crystalline embryos much smaller than critical nuclei.¹⁸ Such polyhedra were also effective in the aforementioned investigation by Swope and Andersen of nucleation in a liquid of Lennard-Jones spheres.¹¹ Because the criteria provided by Voronoi polyhedra appear to be more robust in the identification of the bcc crystals of the hexafluorides than in the case of fcc crystals such as NaCl, an alternative criterion was investigated. An ion and its partners of the same charge in its coordination sphere (Na⁺–Na⁺, or Cl[−]–Cl[−] as the case may be) were considered to be in an fcc packing arrangement if the coordination number was 12 for partners within the distance of the first minimum of the pair correlation function of the pairs involved, namely, 5.5 Å. This criterion is unable to recognize ions in fcc particles smaller than 13 ions of a given kind, however, and is therefore inadequate for detection of aggregates as small as critical nuclei at 500 K according to classical nucleation theory. Nevertheless, it is more sensitive than the configurational energy in monitoring the growth of the solid nuclei once nucleation has taken place. For

this reason it was applied to identify times of nucleation. It detected no fcc nuclei in melts warmer than 920 K and gave no evidence of preexisting critical nuclei in the abruptly cooled systems. Moreover, the orientations of the axes of the crystals nucleated were unrelated to those of the original crystals from which the melt was generated. Hence, it appears that the melts were free from pockets of crystalline nuclei left from the original solid cluster.

The time of nucleation in any run was identified as the time step at which the number of ions found to be in fcc arrangements began a concerted ascent, and the time t_0 , from which the nucleation time was reckoned, was taken to be the time of entry into the cold reservoir (i.e., heat bath at the final temperature).

Interpretation in Terms of Nucleation Theory. Information derivable from the present runs includes nucleation rates at three temperatures. It may become possible in the future to exploit the molecular detail intrinsic in the runs and to determine the sizes and shapes of the critical nuclei responsible for the freezing, but sharper criteria would be required than have been applied in this study. If some form of nucleation theory is adopted, analyses of the nucleation rates can lead to an estimate of the interfacial free energy between the solid nuclei and the surrounding liquid medium. To calculate the nucleation rates, it is necessary to decide what fraction of the cluster volume is effectively available for nucleation. For systems previously treated in this laboratory, the solid nucleated was well-wetted by the molten phase around it. As a consequence, the disordered surface of the solid melted at a significantly lower temperature than the core and conversely, on cooling, freezing of the liquid always began in the interior of a cluster. The surface was not favorable for nucleation. Our convention for a roughly spherical cluster of N molecules has been to calculate the volume of the core, excluding the surface molecules by applying the approximation for F , the fraction of molecules residing in the surface, of

$$F = 3\left(\frac{4\pi}{3N}\right)^{1/3} \left[1 - 0.5\left(\frac{4\pi}{3N}\right)^{1/3}\right]^2 \quad (2)$$

Although this convention of excluding only surface molecules might, at first glance, seem to reject too trivial a fraction of a cluster volume, it excludes fully 70% in a cluster of 108 molecules. Obviously, the arbitrariness in assigning a volume for nucleation in small clusters leads to an appreciable uncertainty. It is minor in comparison with errors as high as factors of 10^5 that are sometimes considered to be tolerable at the present stage of development of nucleation theory.³⁵

Salt clusters are obviously very different from those of simple nonpolar molecules. Their nonwetting characteristics discussed at length by Rose and Berry¹⁹ make a cluster tend to expel a solid aggregate to the surface. The well-faceted right-rectangular shapes of clusters frozen from the melt attest to the strong drive toward order at the 100 surfaces favored during freezing. It is reasonable, then, to suppose that the surface should not be excluded as a site for nucleation. Nevertheless, surface molecules in a melt enjoy fewer neighbors with which to interact cooperatively in the structural fluctuations leading to solid nuclei. We will assume, crudely and speculatively, that surface sites defined as above are only about one-third as likely to be sites of nucleation as interior sites. Accordingly, for a cluster with 108 NaCl ion pairs, we assume that the fraction of volume eligible for nucleation is roughly $[(1 - 0.70) + 0.70/3]$, or about 53%. This crude estimate is likely to be in error by less than a factor of 2. We denote the eligible volume as V_{eff} in the following.

Many variants of classical nucleation theory have been formulated, in most of which the rate is expressed as

$$J = A \exp\left(\frac{-\Delta G^*}{k_B T}\right) \quad (3)$$

where ΔG^* is the free energy barrier to nucleation. Formulations for which the prefactor A is based on jump rates of molecules from the old phase to the new modeled in terms of viscous flow appear greatly to exaggerate the role of viscosity in inhibiting nucleation and growth.^{13,36,37} The most rigorous prefactor we are aware of is that proposed by Grant and Gunton.³⁸ Even though it was derived for monatomic units, we will apply it for want of a better alternative. The prefactor is expressed as

$$A = \kappa \Omega / V \quad (4)$$

where V is the volume of the system, κ is the dynamic prefactor

$$\kappa = \frac{2\lambda\sigma_{sl}T}{L^2R^{*3}} \quad (5)$$

with λ , L , and R^* representing the thermal conductivity, heat of fusion per unit volume of solid, and radius of the critical nucleus, respectively, and Ω is the dimensionless statistical prefactor

$$\Omega = \left(\frac{2}{27^{1/2}}\right) \left(\frac{V}{\xi^3}\right) \left(\frac{\sigma_{sl}\xi^2}{k_B T}\right)^{3/2} \left(\frac{R^*}{\xi}\right)^4 \quad (6)$$

with ξ a small correlation length characterizing the thickness of the interface between the old and new phases. Most of the parameters invoked are reasonably straightforward and are available either for a system governed by the present potential function or from the bulk. To compute the free energy of freezing at the low temperatures of the present runs, a knowledge of the difference in heat capacity between the liquid and the solid is required down to 500 K. Since any extrapolation of the experimental heat capacity of the liquid to 500 K is entirely speculative, the caloric curves of the present MD runs were used for the purpose. We compute R^* from the classical expression

$$R^* = -2\sigma_{sl}/\Delta G_v \quad (7)$$

where ΔG_v is the free energy of freezing per unit volume. The parameter ξ entering the prefactor requires some comment because its magnitude is not readily estimated intuitively and its effect is amplified by its appearance to the fourth power. Correlation lengths for freezing have been estimated by Oxtoby and Harrowell³⁹ for argon and two fcc metals and for silicon. If we associate the Oxtoby–Harrowell lengths, which were based on the variation of free energy with order parameter, with the Grant–Gunton ξ based on the variation of free energy with change in density, it is possible to complete the analysis. For the substances whose solids are fcc, the correlation lengths in angstroms were roughly $0.6v_m^{1/3}$ near the freezing point T_f , where v_m is the liquid volume per molecule. For Si, however, which is structurally very different, the correlation length was over twice that value (making ξ^4 40-fold larger). Results of three other model studies⁴⁰ suggested that the correlation length decreases with supercooling, perhaps as $\sim T^{1.3}$. Although it is risky to relate a salt to a rare-gas solid or metal, it seemed plausible to consider the Cl^- ions close-packed in the fcc lattice of salt to be more similar to fcc materials than to Si. Therefore, speculatively, we took ξ to be $0.6(T/T_f)^{1.3}$ times the cube root

TABLE 3: Physical Properties Adopted for NaCl

property	value	ref
T_m , K	1073	<i>a</i>
ΔH_{fus} , J/mol	30 180 at T_m	<i>a</i>
$C_p(l) - C_p(s)$, J/(mol K)	17.5	this research
V_{sol} , m ³ /mol	26.7×10^{-6}	<i>a</i>
V_{liq} , m ³ /mol	31.4×10^{-6}	47
λ , W/(mK)	$0.10 + 0.0008T$	<i>b</i>
ξ , Å	$2.2(T/T_m)^{1.3}$	see text

^a CRC Handbook of Chemistry and Physics, 63rd ed; CRC Press: Boca Raton, FL, 1982. ^b Smirnov, M. V.; Khokhlov, V. A.; Filatov, E. S. *Electrochim. Acta* **1987**, 32, 1019.

of the volume per Cl⁻ ion. For the free energy barrier in eq 3, the conventional expression^{13,21,41}

$$\Delta G^* = \frac{16\pi\sigma_{sl}^3}{3(\Delta G_v + w')^2} \quad (8)$$

was used, where w' expresses a correction for the work of changing surface area of the cluster as a nucleus forms in the interior, or $(2\sigma_l/r_0)(\rho_l - \rho_s)/\rho_l$, with $2\sigma_l/r_0$ representing the Laplace pressure exerted by the liquid phase on the solid. Such a correction is excessive if nucleation occurs in the surface, but we retain it in this preliminary study. The final parameters adopted in the analysis are listed in Table 3.

Results

Behavior during Heating and Cooling. Figure 1 graphically illustrates the condition of a cluster as it is heated to melting and then frozen. Changes that are evident upon visual inspection are reflected in the various numerical indicators of the gross state of the cluster such as the configurational energy (Figure 2), the Lindemann δ (the ratio of root-mean-square displacements of *adjacent* ions to their mean separations (Figure 3)), and the Na⁺-Cl⁻ pair correlation function (Figure 4). The dark points in Figure 2 show the substantial effects of nonequilibrium associated with the high rates of temperature change initially imposed, and the crosses corresponding to 10-fold longer periods in the heat bath indicate that the melting temperature of (NaCl)₁₀₈ is between 900 and 920 K. Because freezing involves the stochastic process of nucleation, the degree of supercooling in any run depends on chance as well as on the cooling rate.

Nucleation. In the runs designed to determine nucleation rates, the degree of supercooling was established not by chance but by plunging the system into a cold reservoir at 500, 525, or 550 K and keeping it there until it froze. Figures 5 and 6 show the evolution of configurational energy and the number of chloride ions meeting the fcc criterion as a function of time in typical runs. Times of nucleation can be recognized in plots such as those of Figure 5 but are identified more definitively by the onset of a steady increase in the number of ions in fcc configurations (cf. Figure 6). Times of freezing of the individual runs are listed in Table 2, and the decay of the fraction N_0 surviving nucleation is plotted for each temperature in Figure 7. Not all of the clusters froze in the runs at 550 K during the 120 ps of observation. From the slopes of the curves in Figure 7, nucleation rates can be derived via

$$\frac{d \ln N_0}{dt} = -JV_{eff} \quad (9)$$

where V_{eff} is the volume eligible for nucleation according to the criterion described in the foregoing. Nucleation rates

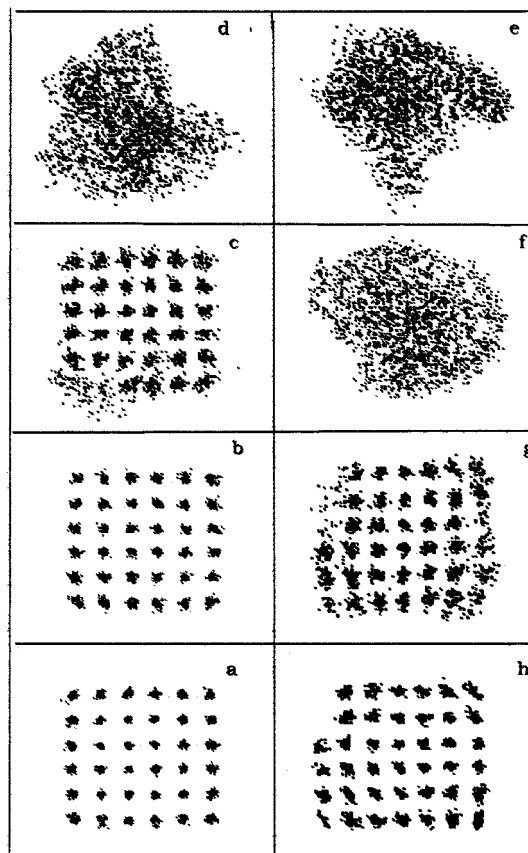


Figure 1. Images of an (NaCl)₁₀₈ cluster at various stages of heating (left-hand column) and cooling (right-hand column): (a) 400, (b) 600, (c) 900, (d) 920, (e) 910, (f) 810, (g) 570, and (h) 410 K. Heating continued to 980 K before cooling began. Orientations of the crystalline clusters were adjusted for visual inspection. Lattice directions after the melt nucleated differed from those before melting.

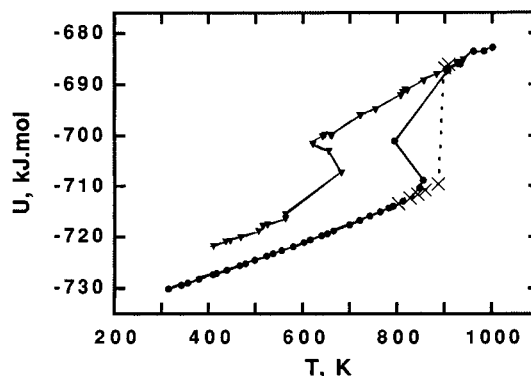


Figure 2. Configurational energy (per mole of NaCl pairs in a cluster) as a function of temperature during the heating (●) and cooling (▼) stages with 1000 time steps. The dashed line and crosses are with 10 000 time steps spent in the heat bath at each temperature. The failure to return to the original configurational energy upon refreezing reflects the failure to recover the original optimal external shape.

inferred from the MD runs were 2.1×10^{37} , 1.5×10^{37} , and $4.9 \times 10^{36} \text{ m}^{-3} \text{ s}^{-1}$ at 500, 525, and 550 K, respectively. These rates are astronomical in comparison with those observed in most prior experimental measurements of nucleation rates but are only a factor of $\sim 10^7$ higher than those implied by the experimental results of Buckle and Ubbelohde at 885 K.²²

When the MD nucleation rates are inserted into the classical expression, values of the kinetic parameter σ_{sl} identified with the interfacial free energy between the liquid and solid could

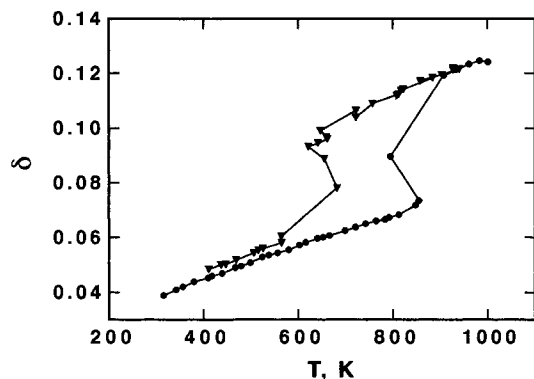


Figure 3. Lindemann indices $\delta(T)$ averaged over all adjacent pairs of ions in a cluster during heating (\bullet) and cooling (\blacktriangledown) stages with 1000 time steps spent in the heat bath at each temperature. Note the similarity to the corresponding configurational energies of Figure 2 except for the lower sensitivity of δ to the external cluster shape.

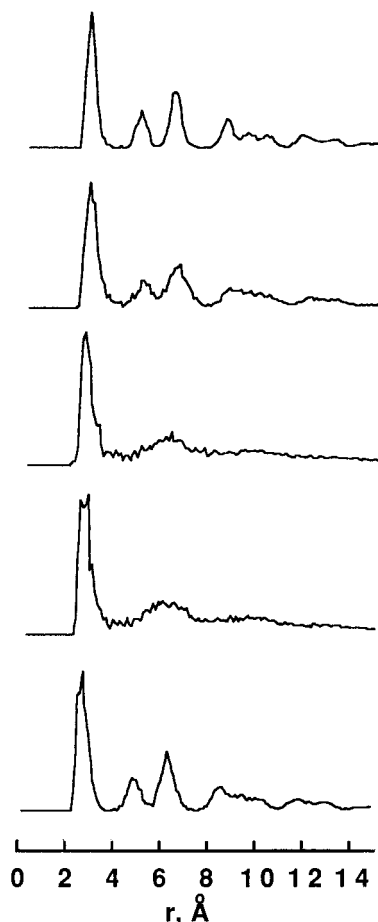


Figure 4. Na-Cl pair-correlation functions at various temperatures during heating and cooling stages. From top to bottom, the temperatures are the following: (heating) 400, 800, and 920 K; (cooling) 810 and 410 K.

be calculated. They were found to be 117.7, 117.6, and 119.6 mJ/m^2 at 500, 525, and 550 K, respectively. If the rate-enhancing correction w' had been ignored in eq 8, the interfacial free energies would have been about 8% smaller. If the uncertainties in the nucleation rates were assumed to be due solely to the statistics of chance events (an underestimation, of course) and that these constitute the only uncertainty in σ_{sl} , then the standard deviations of the interfacial free energies would be about 1%. Flaws in nucleation theory lead to far greater uncertainties than this.

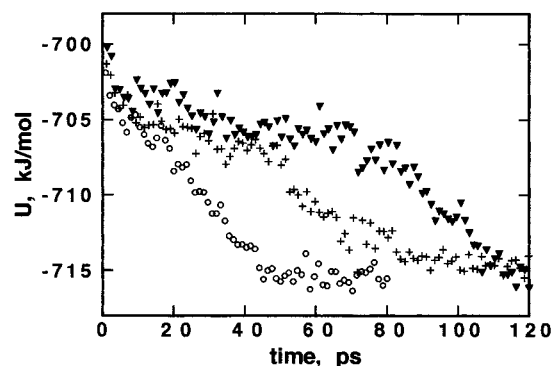


Figure 5. Time evolution of the configurational energies in typical nucleation runs at 500 K (\circ), 525 K ($+$), and 550 K (\blacktriangledown).

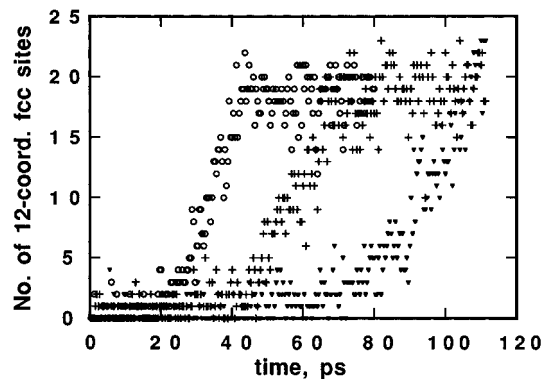


Figure 6. Time evolution of the number of chloride ions at 12-coordinate sites meeting the criterion considered to characterize crystalline fcc sites. Results from typical nucleation runs are at 500 K (\circ), 525 K ($+$), and 550 K (\blacktriangledown).

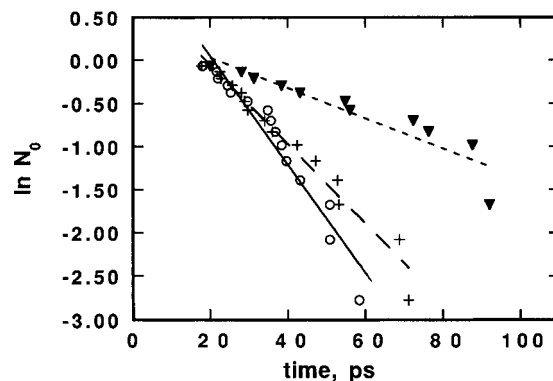


Figure 7. Decay of population of liquid clusters with time from 16 MD runs each at 500 K (\circ), 525 K ($+$), and 550 K (\blacktriangledown)

Discussion

Removing Heat of Fusion. First, we comment on our decision to keep clusters in a heat bath during the entire period of nucleation and growth. The main reason was to maintain a nearly isothermal environment. In research on the freezing of other systems maintained at constant energy, the heat of fusion released into small clusters has caused extremely irregular behavior. Sometimes a cluster that had already spontaneously frozen almost entirely (and had certainly attained a size far larger than that of a critical nucleus) would then almost completely melt.⁴² Although isothermal MD techniques have been introduced by Nosé⁴³ and used successfully, we were concerned with the possibility that their constraints might interfere with the dynamic evolution of nucleation (as well as add complexity to an already computer-intensive study). On the other hand, when a simple heat bath is used to control the temperature, the

algorithm removes the heat of fusion liberated, cooling the warmest sites more rapidly than their cooler surroundings. Such an effect is similar to the diffusion of heat from a nucleation site, which would have occurred if the system had been much larger and therefore less vulnerable to the evolution of heat on freezing.

Diagnostic Indicators. Several points illustrated by the figures deserve comment. In Figure 1 can be seen the irregular shapes of the liquid clusters and the conspicuous 100 facets of the clusters that have resolidified. The latter is very different in aspect from those of frozen clusters of the simple, nonpolar substances we have encountered. The softer materials have a lower drive to minimize surface free energies than do the hard salts. On the other hand, the curious shapes of the liquid clusters can be accounted for quantitatively by thermally excited capillary waves,⁴⁴ a manifestation of internal Brownian motion. Here, surface tension is insufficient to suppress the surface waves and draw a cluster up into a sphere.

In Figures 2 and 3 are shown the close parallel between the Lindemann index and the configurational energy. This is a consequence of the fact that for classical harmonic oscillators the mean-square displacement is proportional to the mean potential energy. Since molecules oscillating in the cages of their neighbors execute roughly harmonic motions, the similarity of $\delta(T)$ in Figure 3 to $U(T)$ in Figure 2 is natural, even in the regions well out of equilibrium in partial melting and in supercooling. For atomic clusters it has been found that melting is associated with an increase of δ to about 0.1. Melting of the present NaCl clusters appears to take place at a rather lower index, and indices of the supercooled liquid clusters fell somewhat below 0.1.^{29,31,32}

Conformity with Nucleation Theory. According to classical nucleation theory,^{22,40} a steady state of precritical embryos must be established in an isothermal ensemble before nucleation can take place. There can be a significant time lag before this steady state is developed, but the existing distribution of embryos at the initial time of observation can drastically alter this lag. If the time lag is calculated via the well-regarded formulations of Kashchiev⁴⁵ or of Wu,⁴⁶ calculated times before nucleation are enormously longer than those seen in Figure 6. Therefore, it can be concluded that the preexisting embryos facilitate nucleation in the rapidly quenched melts (which are supercooled considerably further than in conventional studies). In Figure 6 can be seen fluctuations in the number of chloride ions calculated to have fcc coordination prior to the onset of concerted growth. These fluctuations are undoubtedly associated with the chance formation and dissolution of embryos. Because the coordination criterion is somewhat too coarse to characterize precritical nuclei properly, a reliable determination of the size of critical nuclei must await further analysis. The plots do suggest weakly, however, that critical nuclei may be somewhat larger than the six chloride ions suggested by classical theory at 500 K. At lower degrees of supercooling critical nuclei are much larger. Those of Buckle and Ubbelohde²² at 885 K approach 100 chloride ions, again, according to classical theory.

Because there is no opportunity for heterophase impurities to catalyze nucleation in the simulations, freezing must be due either to homogeneous nucleation or to spinodal decomposition. The latter phenomenon would start to precipitate solid particles throughout the supercooled melt at once and tend to produce polycrystalline clusters. This chaotic behavior was not observed. The statistics of the timing of the stochastic events was in good accord with that expected from homogeneous nucleation, and furthermore, each freezing event led to a single crystal. We

conclude, then, that the observed behavior of highly supercooled clusters of salt is in at least qualitative agreement with classical nucleation theory except for the very short time lags seen. The preparation of the samples, however, was not such that theoretical predictions of time lags could be tested quantitatively.

Interfacial Free Energy. The interfacial free energies σ_{sl} of 117.7, 117.6, and 119.6 mJ/m² derived from the nucleation rates at 500, 525, and 550 K, respectively, are of the same order of magnitude as the value of 84.1 mJ/m² at 885 K reported by Buckle and Ubbelohde.²² These authors used a different variant of nucleation theory, did not measure nucleation rate, and derived σ_{sl} from a crudely estimated nucleation time lag of 10 s together with “representative values” of molar volumes and activation energies of self-diffusion for salts in general.

Our interfacial free energy at 500 K is substantially lower than the linearly extrapolated surface tension of the liquid⁴⁷ of ~155 mJ/m² as expected from Neumann’s rule according to the analysis of Buckle and Ubbelohde.²² A decrease of surface tension with temperature is characteristic of liquids. Whether the apparent small increase in our σ_{sl} values with temperature is real is uncertain, but Turnbull⁴⁸ and Spaepen⁴⁹ have both argued that the interfacial free energy is likely to rise with T because of the negative excess interfacial entropy of the interface. Solid surfaces tend to be rigid, forcing a liquid in contact with the solid to organize into a more ordered structure than in the bulk in order to conform to the interface. Although this rationale is very plausible, virtually no precise data exist to support (or negate) the argument. The sole example meeting all of Turnbull’s criteria⁵⁰ for homogeneous nucleation and believed to give $\sigma_{sl}(T)$ with sufficient accuracy to establish the positive sign of $d\sigma_{sl}(T)/dT$ is that of Turnbull’s 1952 investigation of the freezing of mercury.⁵⁰

It is of some interest to compare the σ_{sl} values derived from the present MD simulations with the values predicted from an empirical relation due to Turnbull,⁵¹ wherein

$$\sigma_{sl} \approx \frac{k_T \Delta \bar{H}_{fus}}{(\bar{V}^2 N_A)^{1/3}} \quad (10)$$

with \bar{V} the molar volume (whether of the solid or liquid was not specified) and k_T a constant found to be ~0.32 for a series of metalloids and nonmetals and 0.45 for metals. Interfacial free energies to calibrate eq 10 were derived from nucleation kinetics. Since no salts had been studied, it is not known whether a similar value for k_T applies to them. If we adopt 0.32 for the constant, the heat of fusion at the melting point, and the liquid volume, eq 10 gives 115 mJ/m², a value close to that from the MD simulations. A somewhat larger value would have been calculated from the heat of fusion at 500 K and molar volume of the solid.

Thickness of Interface. One feature marring the classical nucleation theory is its disregard of the diffuseness of the interface between the two phases involved. The interface is treated as if it has an infinitesimal thickness. Only one generally applicable theory (i.e., theory requiring no more data for its application than the classical theory) has been formulated explicitly to take the diffuseness into account. That is the diffuse interface theory (DIT) of Granasy.^{52–54} Whereas the key governing parameter in the classical nucleation theory (CNT) is the interfacial free energy σ_{sl} , the characteristic parameter in the DIT is its thickness δ . This parameter has as yet no known relation to the Tolman thickness,⁵⁵ δ , or to the correlation distance ξ met in the Grant–Gunton³⁸ and density functional treatments.³⁹ Values of the Granasy parameter δ derived from

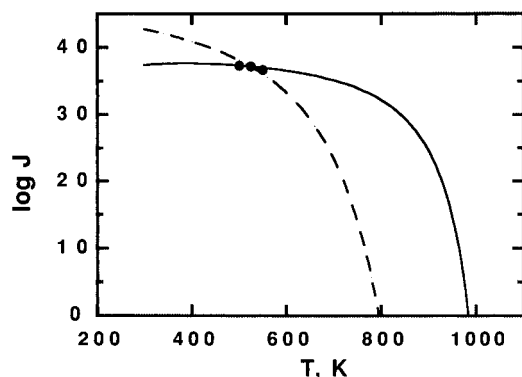


Figure 8. Temperature dependence of nucleation rate ($\text{m}^{-3} \text{s}^{-1}$) according to the classical nucleation theory with constant σ_{sl} (solid curve) and Granasy's diffuse interface theory with constant δ (dashed curve). Points represent rates from MD runs.

the present nucleation data were 2.35, 2.21, and 2.12 Å, each with purely statistical errors of ~ 0.03 Å at 500, 525, and 550 K, respectively. A comparison of these values with the radius of the critical nucleus $R^* \approx 4$ Å calculated from the CNT augurs poorly for the classical theory. Whatever may be the physical meaning of δ and the correlation length, $\xi \approx 0.8\text{--}2$ Å as estimated above, their values are so large in comparison with the classical value of R^* as to raise considerable doubt about the classical theory. According to Granasy, δ is expected to be independent of temperature (except for the case of water,⁵⁴ which appears to consist of a mixture of structures whose proportions are temperature-dependent⁵⁶). Granasy assigns an effective interfacial free energy, σ_{eff} , to make the classical ΔG^* value equal to ΔG^* for the DIT. It is of interest to note, then, that a constant δ implies that σ_{eff} increases with temperature qualitatively as suggested by Turnbull⁴⁸ and Spaepen.⁴⁹ On the other hand, taking the DIT and classical values of ΔG^* to be the same guarantees that the values of σ_{eff} derived from the present nucleation rates are identical with the σ_{sl} values reported above. Granasy asserts that a prime difference between the CNT and DIT is the adoption of an essentially constant σ_{sl} in the former and a constant δ in the latter. It is informative, then, to compare the temperature dependence of nucleation rates according to CNT and DIT under these constraints. This is shown in Figure 8. Unfortunately, the present MD runs are too closely spaced to suggest a preference. If it is legitimate to compare the experimental system of Buckle and Ubbelohde^{20,22} with our computational model, the experimental results at 885 K are closer to the CNT curve than to the DIT curve, and by an overwhelming margin. On the other hand, the drastic assumptions in the interpretation of experiments together with the absolutely enormous disparity in the sizes of the systems make the conclusion less than decisive.

Supersonic Experiments. Because of the ability of the supersonic technique, when applicable, to measure nucleation rates directly, it would be of some interest to decide between the two curves of Figure 8 and to resolve the questions raised in the previous paragraph by the new experimental method. A problem in performing the experiments is the limitation of the supersonic technique at its present stage of development to temperatures in the vicinity of the so-called evaporative cooling temperature, T_{evp} .^{57,58} Several rules of thumb^{13,58} to estimate this temperature suggest that it is not far from the temperature of the Buckle–Ubbelohde investigation at 885 K.²² Taking into account the typical size of the clusters involved and the observation times of microseconds up to some dozens of microseconds, nucleation rates must be of the order of 10^{28} –

$10^{30} \text{ s}^{-1} \text{ m}^{-3}$ to be accessible to measurement. Therefore, if the CNT curve of Figure 8 were more or less valid, salt clusters are promising subjects. This assumes that the nucleation time lag would not be longer than has been characteristic in experiments with supersonic jets. The apparently very large lag of the Buckle–Ubbelohde experiments would be fatal. On the other hand, if the DIT curve is correct, it would be hopeless to carry out the supersonic experiments unless an effective means of controlled temperatures of clusters in a supersonic jet were devised.

Concluding Remarks

Clusters of salt behave very differently from van der Waals clusters of nonpolar molecules according to the present molecular dynamics simulations. Surface melting is much less pronounced, making the melting transition much sharper. The impetus to form large facets on crystallizing is much more pronounced. Consistent with the results of van der Waals clusters, however, was the qualitative adherence of nucleation rates of highly supercooled liquid clusters to the classical theory of homogeneous nucleation and the agreement of the derived interfacial free energy parameter σ_{sl} with Turnbull's empirical relation.⁵¹ This parameter was also in rough agreement with an experimental value of the interfacial free energy at a much lower degree of supercooling derived on a very different basis.²² The simulations weakly suggested an increase in σ_{sl} with temperature, a tendency consistent with a proposal of Turnbull⁴⁸ and Spaepen.⁴⁹ Nevertheless, indicators of the thickness of the interface between the solid and its melt derived from Granasy's diffuse interface theory⁵² and estimated from density functional calculations by Oxtoby and co-workers^{39,40} suggest that the thickness is comparatively large. It is such an unacceptably large fraction of the classical critical radius as to suggest that the classical theory must, at best, be only qualitatively applicable to our small clusters. Analyses of critical nuclei in MD simulations to establish their sizes and to map the region of structural transition at their interface with the melt should be helpful for future formulations of treatments of nucleation. Further simulations on larger clusters over a much wider temperature range should decide between alternatives illustrated in Figure 8 and should indicate the likelihood that salt clusters can be investigated by the new experimental technique of supersonic expansion.

Acknowledgment. This research was supported by a grant from the National Science Foundation. We thank Professor David Oxtoby for helpful discussions about the correlation length.

References and Notes

- (1) Turnbull, D. *J. Appl. Phys.* **1949**, *20*, 817.
- (2) Turnbull, D. *J. Met.* **1950**, *188*, 1144.
- (3) Turnbull, D.; Cech, R. E. *J. Appl. Phys.* **1950**, *21*, 804.
- (4) See the following. Cargill, G. S.; Spaepen, F.; Tu, K.-N., Eds. *Phase Transitions in Condensed Systems—Experiments and Theory* (Turnbull Festschrift); Materials Research Society: Pittsburgh, PA, 1987.
- (5) Bartell, L. S.; Dibble, T. S. *J. Am. Chem. Soc.* **1990**, *112*, 890; *J. Phys. Chem.* **1991**, *95*, 1159.
- (6) Dibble, T. S.; Bartell, L. S. *J. Phys. Chem.* **1992**, *96*, 2317.
- (7) Huang, J.; Bartell, L. S. *J. Phys. Chem.* **1994**, *98*, 4543; *J. Phys. Chem.* **1995**, *99*, 3924.
- (8) Huang, J.; Lu, W.; Bartell, L. S. *J. Phys. Chem.* **1995**, *99*, 11147.
- (9) Huang, J.; Lu, W.; Bartell, L. S. *J. Phys. Chem.* **1996**, *100*, 14276.
- (10) Dibble, T. S.; Bartell, L. S. *J. Phys. Chem.* **1992**, *96*, 8603.
- (11) Swope, W. C.; Andersen, H. C. *Phys. Rev. B* **1990**, *41*, 7042.
- (12) Bartell, L. S.; Xu, S. *J. Phys. Chem.* **1991**, *95*, 8939.
- (13) Bartell, L. S. *J. Phys. Chem.* **1995**, *99*, 1080.

- (14) Raoult, B.; Farges, J.; de Feraudy, M. F.; Torchet, G. *Z. Phys. D* **1989**, *12*, 85; *Philos. Mag. B* **1989**, *60*, 881.
- (15) Bartell, L. S.; Xu, S. *J. Phys. Chem.* **1995**, *99*, 10446.
- (16) See, for example, the literature cited in ref 11.
- (17) Bartell, L. S.; Xu, S. *J. Phys. Chem.* **1994**, *98*, 6688.
- (18) Kinney, K.; Xu, S.; Bartell, L. S. *J. Phys. Chem.* **1996**, *100*, 6935.
- (19) Rose, J. P.; Berry, R. S. *J. Chem. Phys.* **1993**, *98*, 3262.
- (20) Buckle, E. R.; Ubbelohde, A. R. *Proc. R. Soc. London, Ser. A* **1960**, *529*, 325.
- (21) Buckle, E. R. *Proc. R. Soc. London, Ser. A* **1961**, *261*, 189.
- (22) Buckle, E. R.; Ubbelohde, A. R. *Proc. R. Soc. London, Ser. A* **1961**, *261*, 197.
- (23) Luo, J.; Landmann, U.; Jortner, J. In *Physics and Chemistry of Small Clusters*; Jena, P., Rao, B. K., Khanna, S., Eds.; NATO ASI Series B 158; Plenum: New York, 1987; p 210.
- (24) Fincham, D.; Anastasiou, N. *MDIONS*; CCP5 Program Library; SERC Daresbury Laboratory: Daresbury, U.K., 1981, revised 1994.
- (25) Born, M.; Mayer, J. E. *Z. Physik* **1932**, *75*, 1.
- (26) Huggins, M. L.; Mayer, J. E. *J. Chem. Phys.* **1933**, *1*, 643. Huggins, M. L. *J. Chem. Phys.* **1937**, *5*, 643.
- (27) Tosi, M. P.; Fumi, F. *J. Phys. Chem. Solids* **1964**, *25*, 45.
- (28) Westman, R.; Magneli, A. *Acta Chem. Scand.* **1957**, *11*, 1587.
- (29) Eters, R. D.; Kaelberer, J. B. *J. Chem. Phys.* **1977**, *66*, 3233; *Phys. Rev. A* **1975**, *11*, 1068.
- (30) Lindemann, F. A. *Phys. Z.* **1910**, *11*, 609; *Engineering* **1912**, *94*, 515.
- (31) Davis, H. L.; Jellinek, J.; Berry, R. S. *J. Chem. Phys.* **1987**, *86*, 6456.
- (32) Beck, T. L.; Jellinek, J.; Berry, R. S. *J. Chem. Phys.* **1987**, *87*, 545.
- (33) Tanemura, M.; Hiwatari, Y.; Matsuda, H.; Ogawa, T.; Ogita, N.; Ueda, A. *Prog. Theor. Phys.* **1977**, *58*, 1079.
- (34) Cape, J. N.; Finney, J. L.; Woodcock, L. V. *J. Chem. Phys.* **1981**, *5*, 2366.
- (35) Oxtoby, D. W. Sixth International Symposium on Small Particles and Inorganic Clusters, Chicago, September 1992.
- (36) Oxtoby, D. W. Private communication, 1994.
- (37) Burke, E.; Broughton, Q.; Gilmer, G. H. *J. Chem. Phys.* **1988**, *89*, 1030.
- (38) Grant, M.; Gunton, J. D. *Phys. Rev. B* **1985**, *32*, 7299.
- (39) Oxtoby, D. W.; Harrowell, P. *J. Chem. Phys.* **1992**, *96*, 34.
- (40) Harrowell, P.; Oxtoby, D. W. *J. Chem. Phys.* **1984**, *80*, 1639. Shen, Y. C.; Oxtoby, D. W. *J. Chem. Phys.* **1996**, *104*, 4233; *J. Chem. Phys.* **1996**, *105*, 6517.
- (41) Turnbull, D.; Fisher, J. C. *J. Chem. Phys.* **1949**, *17*, 71.
- (42) Santikary, P.; Bartell, L. S. Unpublished research.
- (43) Nosé, S. *Mol. Phys.* **1984**, *52*, 255; *J. Chem. Phys.* **1984**, *81*, 511.
- (44) Bartell, L. S. *J. Mol. Struct.*, in press; *Surf. Sci.*, in press.
- (45) Kashchiev, D. *Surf. Sci.* **1969**, *14*, 209.
- (46) Wu, D. *J. Chem. Phys.* **1992**, *97*, 9622.
- (47) *International Critical Tables of Numerical Data, Physics, Chemistry and Technology*; McGraw-Hill: New York, 1926–1939.
- (48) Turnbull, D. In *Physics of Non-Crystalline Solids*; Prins, J. A., Ed.; North-Holland: Amsterdam, 1964; p 4.
- (49) Spaepen, F. *Acta Metall.* **1975**, *23*, 729.
- (50) Turnbull, D. *J. Chem. Phys.* **1952**, *20*, 411.
- (51) Turnbull, D. *J. Appl. Phys.* **1950**, *21*, 1022.
- (52) Granasy, L. *J. Non-Cryst. Solids* **1993**, *162*, 301. Note that no correction for the effect of the Laplace pressure of the melt on the nucleation rate has been incorporated in the DIT formalism. It was also ignored in the present DIT computations. Moreover, Granasy has used an earlier variant of the prefactor based on self-diffusion rather than that of ref 38. In the present paper, however, we have adopted the Grant–Gunton prefactor to derive Granasy's parameter δ and to construct Figure 8. The strong temperature dependence of ξ^4 that we have incorporated in the prefactor yields a steeper DIT plot than Granasy's prefactor would have given.
- (53) Granasy, L. *Mater. Sci. Eng. A* **1994**, *178*, 121.
- (54) Granasy, L. *J. Phys. Chem.* **1995**, *99*, 14182.
- (55) Tolman, R. C. *J. Chem. Phys.* **1949**, *17*, 333.
- (56) Bartell, L. S. *J. Phys. Chem. B* **1997**, *101*, 7573.
- (57) Gspann, J. In *Physics of Electronic and Atomic Collisions*; Datz, S., Ed.; North-Holland: New York, 1982.
- (58) Klots, C. E. *J. Phys. Chem.* **1988**, *92*, 5864.